AFOSR-TR-97

0524

REPORT DOCUMENTATION PAGE

1. AGENCY USE ONLY (Leave blank)	2. REPORT DATE	3. REPORT TYPE AND DATES COVERED
		FINAL TECHNICAL 15 AUG 93 - 31 AUG 97

4. TITLE AND SUBTITLE

TRANSPORT OF AIR PLASMAS

5. FUNDING NUMBERS

61102F
2301/ES

6. AUTHOR(S)

PROFESSOR KRUGER

7. PERFORMING ORGANIZATION NAME(S) AND ADDRESS(ES)

THE BOARD OF TRUSTIEES OF THE LELAND
STANFORD JUNIOR UNIVERSITY
857 SERRA STREET ROOM 260
STANFORD CA 94305-4125

8. PERFORMING ORGANIZATION REPORT NUMBER

9. SPONSORING/MONITORING AGENCY NAME(S) AND ADDRESS(ES)

AFOSR/NE

110 DUNCAN AVENUE ROOM B115
BOLLING AFB DC 20332-8050

10. SPONSORING/MONITORING AGENCY REPORT NUMBER

F49620-94-1-0052

11. SUPPLEMENTARY NOTES

12a. DISTRIBUTION/AVAILABILITY STATEMENT

APPROVED FOR PUBLIC RELEASE: DISTRIBUTION UNLIMITED

12b. DISTRIBUTION CODE

13

Several optical diagnostic techniques were developed to interrogate important plasma parameters including temperatures and species concentrations. In particular, a new technique of electron number density measurements based on measurements of the nonequilibrium population of the predissociative C state of NO was devised. ~~The results obtained over the past year are presented in this report.~~ It was found that the three-body NO recombination rate proposed by Dunn and Kang appears to be too slow by a factor ~100, and that the rate proposed by Gupta et al. or Park is also too slow, by about a factor ~10. This result has significant implications for the development of techniques to create and maintain elevated electron number densities in air plasmas.

14. SUBJECT TERMS

15. NUMBER OF PAGES

16. PRICE CODE

17. SECURITY CLASSIFICATION OF REPORT	18. SECURITY CLASSIFICATION OF THIS PAGE	19. SECURITY CLASSIFICATION OF ABSTRACT	20. LIMITATION OF ABSTRACT
UNCLASSIFIED	UNCLASSIFIED	UNCLASSIFIED	UL

NSN 7540-01-280-5500

Standard Form 298 (Rev. 2-89)
Prescribed by ANSI Std. 239-18

TRANSPORT OF AIR PLASMAS

FINAL
~~Annual Progress~~ Report Submitted to
Dr. Robert J. Barker
Air Force Office of Scientific Research

Grant No. F49620-94-1-0052

Submitted by

Professor Charles H. Kruger
Principal Investigator

September 1997

HIGH TEMPERATURE GASDYNAMICS LABORATORY
Mechanical Engineering Department
Stanford University

1. Contents

Section **Page**

2. Status of Effort

The goals of this research program are to provide a detailed understanding of the recombination mechanism of atmospheric pressure air plasmas and to assess the reaction rates proposed in the literature. During previous years of this program, it was determined that overall plasma recombination is mostly controled by the rate of a single reaction, the three-body recombination of NO. Experiments with a recombining air/argon plasma were then designed in order to provide an assessment of this key rate. Several optical diagnostic techniques were developed to interrogate important plasma parameters including temperatures and species concentrations. In particular, a new technique of electron number density measurements based on measurements of the nonequilibrium population of the predissociative C state of NO was devised. The results obtained over the past year are presented in this report. It was found that the three-body NO recombination rate proposed by Dunn and Kang appears to be too slow by a factor ~100, and that the rate proposed by Gupta et al. or Park is also too slow, by about a factor ~10. This result has significant implications for the development of techniques to create and maintain elevated electron number densities in air plasmas.

3. Accomplishments/New Findings

3.1. Background

As discussed in our previous progress reports, electron recombination in atmospheric pressure air plasmas at temperatures between 4,500 and 7,500 K occurs primarily through fast and equilibrated two-body dissociative recombination reactions, mainly:

$$NO^+ + e \Leftrightarrow N + O, \quad (1)$$

and therefore the extent of ionizational nonequilibrium under these conditions is governed by the rates of the (slow) neutral recombination reaction,

$$N + O + M \rightarrow NO + M. \quad (2)$$

Thus, the rate of Reaction (2) determines the extent of ionizational nonequilibrium in air plasmas. Yet, very large discrepancies exist in the rate proposed for this reaction by various authors, namely Dunn and Kang,[1] Gupta et al.,[2] and Park.[3,4] The rate proposed by Park is somewhat greater than the rate of Gupta et al., which is itself greater than Dunn and Kang's rate by a factor 10.

To assess the predictions of three air kinetics mechanisms,[1-4] experiments were conducted with recombining atmospheric pressure air plasmas generated with the 50 kW inductively coupled radio frequency plasma torch described in our previous progress reports. Initially in equilibrium at a temperature of 7,160 K, the plasma was cooled to ~4,900 K within ~400 μs by flowing at velocities approaching 0.5 km/s through water-cooled, brass test-sections mounted on the plasma torch nozzle exit. Through detailed

measurements of temperatures, electron number densities, and emission spectra, it was possible to conclude that the rate of Reaction 2 should be faster than the rates proposed by Dunn and Kang and Gupta *et al.*, and at least as fast as the rate proposed by Park.

To provide a better assessment of the rate of Reaction 2 (on which the pure air studies permitted us to place a lower limit), and to extend the range of our previous work to lower temperatures, experiments were conducted with a ~10% air - 90 % argon plasma (15.6 slpm air, 162 slpm argon, and 2.3 slpm H_2) cooled from 7,900 K to approximately 2,500 K over a time of ~1.3 ms and a distance of 65 cm. The small quantity of H_2 was premixed into the gas for purposes of electron number density measurements. Dilution of ~10% air in argon causes the recombination of nitrogen atoms to be about one order of magnitude slower than in the pure air plasma case as the third body efficiency of argon in Reaction 2 is approximately 20 times smaller than the third body efficiencies of N and O atoms. By slowing the overall N atom recombination, it should be possible to observe significant chemical and ionizational nonequilibrium, and thus to place an upper limit on the rate of Reaction 2. Even at this relatively high dilution level, the electron recombination path remains the same as in pure air because electrons still recombine preferentially via the dissociative recombination reaction $NO^+ + e \rightarrow N + O$, even though NO^+ is no longer the dominant ion here.

3.2. Air/Argon recombination experiments

In this section, the results of our experimental studies with an air/argon plasma are presented and discussed. For these measurements, optical emission was collected at the exit of test sections ranging from 0 cm (nozzle exit) to 65 cm in length. As the temperature varies from ~8000 K at the nozzle exit to ~2500 K at the 65 cm test section exit, several different techniques were developed to obtain temperatures and electron number densities at these locations.

<u>0, 10, and 15 cm.</u>

At these locations, the plasma temperature was sufficiently high to obtain temperature profiles from the Abel-inverted line intensities of oxygen (777.3 nm), argon (763.5 nm) and hydrogen (H_α). At each location, the temperatures determined from the three atomic lines were found to agree within 150 K. The temperature profiles measured at 0, 10 and 15 cm are shown in Fig. 1.

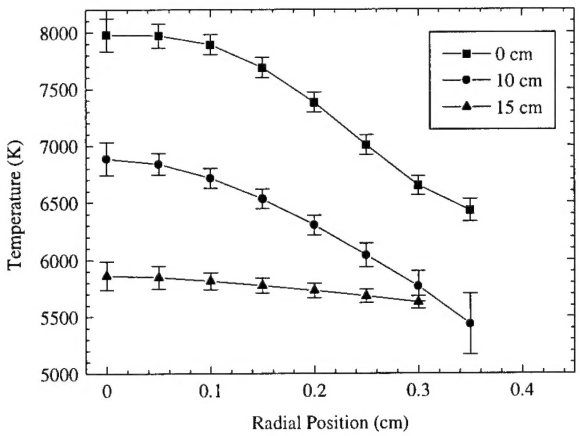

Figure 1. Temperature profiles of the air/argon plasma at 0, 10, and 15 cm downstream of the nozzle exit.

The centerline temperature at these locations is also sufficiently high that a spectrally resolved measurement of the H_β line shape, and thereby of the electron number density,[5] can be obtained. The measured electron number densities match the LTE number densities (Fig. 2) based on the measured centerline temperatures at 0 and 10 cm. At 15 cm, an electron overpopulation of ~3 is measured.

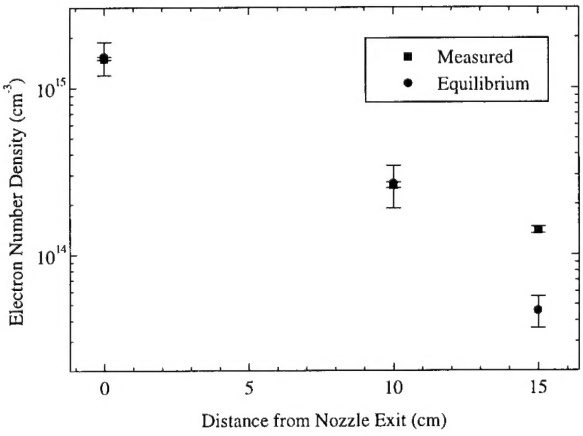

Figure 2. Equilibrium and measured electron number densities (air/argon plasma).

Figure 3 shows comparisons between the equilibrium line-of-sight spectral simulations based on measured temperature profiles and the measured line-of-sight emission spectra. The high centerline temperatures at these locations necessitate consideration of the small but noticeable contribution of the electron recombination continuum to the measured spectra. Due to the uncertainties of accurately calculating this continuum over the measured temperature and wavelength regimes, the continuum is modeled with a constant value added to the NEQAIR2 simulations such that the computations and measurements match at 360 nm. These small additive constants are 10, 0.7, and 0.1 $\mu W/cm^2/sr$ at the 0, 10, and 15 cm locations, respectively. As discussed in Appendix A, these values are consistent with estimates of the argon recombination continuum.

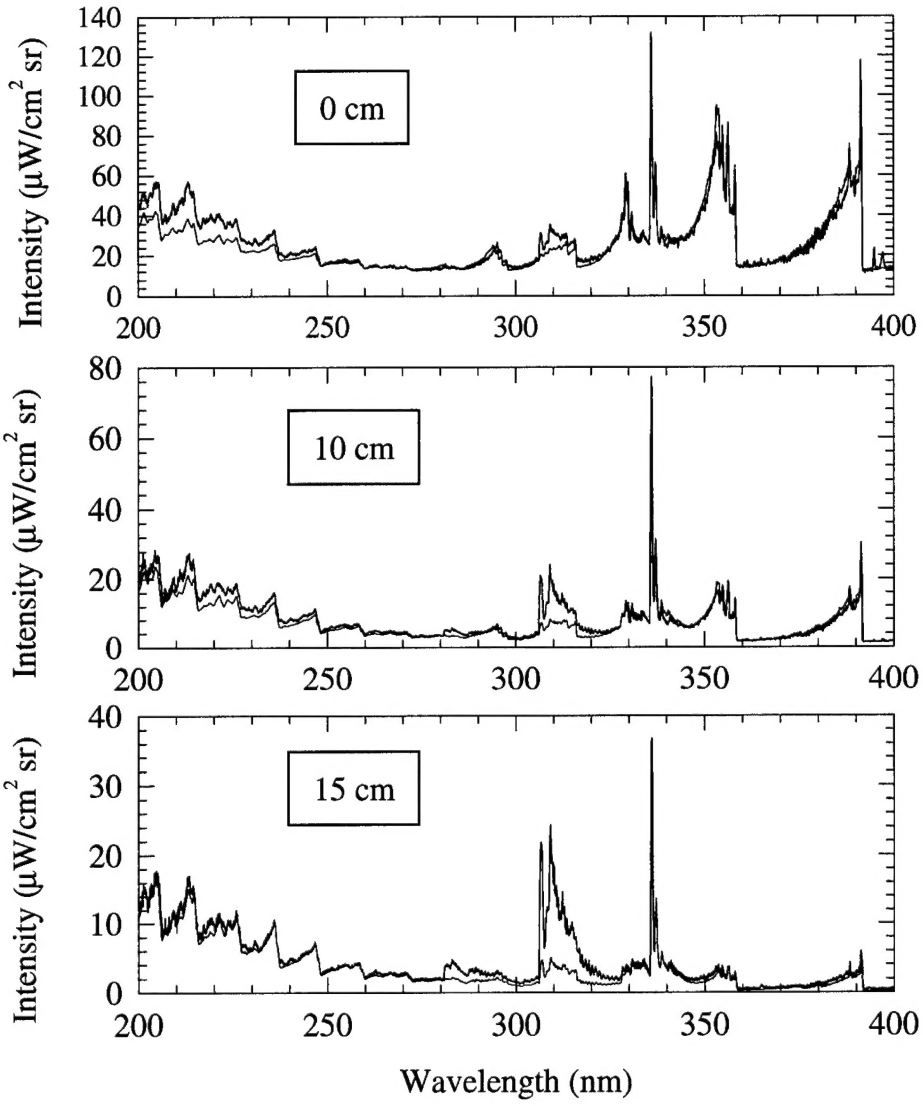

Figure 3. Measured and computed LTE emission spectra of the air/argon plasma at 0, 10 and 15 cm.

As can be seen in Fig. 3, the line-of-sight emission spectra at 0, 10, and 15 cm are reproduced within the 20% experimental uncertainty by equilibrium spectral simulations at the measured temperatures at almost all wavelengths. At 0 cm, the disparity between the two curves near 200 nm is attributed to the inaccuracy in the assumption of a constant electron recombination continuum. Both the argon continuum model and the empirically determined additive constants show a strong dependence on electron number density and a weaker dependence on temperature. As the electron number density and temperature decrease with distance from the nozzle exit, the magnitude of the continuum becomes negligible in comparison with molecular radiation.

At all three locations, the absolute intensity of the OH A $^2\Sigma^+ \rightarrow$ X $^2\Pi_i$ band ($280<\lambda<315$ nm) is not well reproduced by the spectral simulations. This discrepancy can be explained by considering the LTE number density of the OH A state (Fig. 4) which has a maximum at approximately 3700 K, well below all temperatures at a radius of 0.35 cm. The discrepancy therefore arises as the measured OH emission at the 0, 10, and 15 cm locations originates in the outer edges ($r > 0.4$ cm) of the plasma where the Abel-inverted atomic line intensities are too weak to provide reliable temperature information for the spectral simulations.

In summary, at 0 and 10 cm all measurements are consistent with LTE. At 15 cm, the spectral emission is also consistent with LTE despite the small measured electron overpopulation.

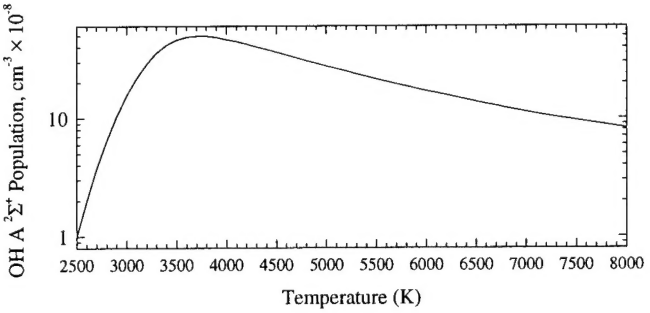

Figure 4. LTE OH A state concentration for the air/argon plasma.

40, 50, 65 cm

At these locations, the excited state populations of atomic species are so small that atomic lines cannot be seen in emission. However, the temperatures can still be accurately deduced by examining the temperature sensitive shape of the measured OH $A^2\Sigma^+ \rightarrow X^2\Pi_i$ band. In particular, the relative strengths of the two peaks at 306.8 and 309.2 nm strongly depend on rotational temperature as both peaks belong to the (0,0) band. The decrease in intensity beyond 311 nm is sensitive to both vibrational and rotational temperatures. As the centerline temperature for these locations was found to be less than 3700 K, the modeling of the measured line-of-sight OH $A^2\Sigma^+ \rightarrow X^2\Pi$ emission spectra does not encounter the difficulties discussed previously.

The centerline temperature is determined by comparing numerical OH spectra[6] at various temperatures normalized to the 309.2 nm peak to the measured line of sight spectra. This shape-matching technique yields centerline temperatures with an accuracy of ~200 K. The remainder of the temperature profile is obtained from the Abel-inverted intensity of the 306.8 peak relative to the 304 nm baseline. The measured line-of-sight OH spectrum at 40 cm is compared with the synthetic spectrum in Fig. 5. The agreement between the *absolute* calculated and measured intensities is typical of all locations.

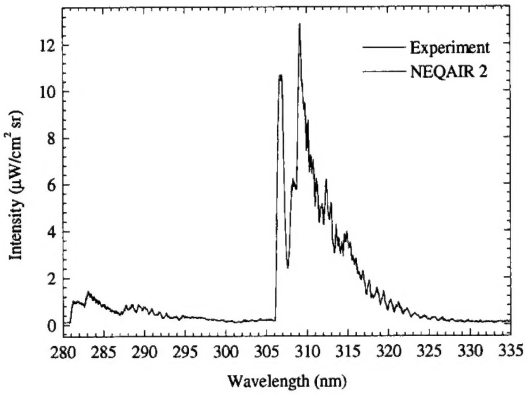

Figure 5. Comparison of measured and calculated line-of-sight OH A→X band at 40 cm (air/argon plasma).

At 50 and 65 cm this procedure must be slightly modified as the plasma was found to be in chemical and ionizational nonequilibrium. The shape of the measured spectra still determines the centerline temperature. However, an overpopulation factor for the OH A state ($\rho_{OH\ A}$) must be determined such that the numerical and measured line-of site spectra agree absolutely. This method, of course, assumes that the overpopulation factor is uniform across the plasma. The OH temperature profiles so determined are displayed in Fig. 6.

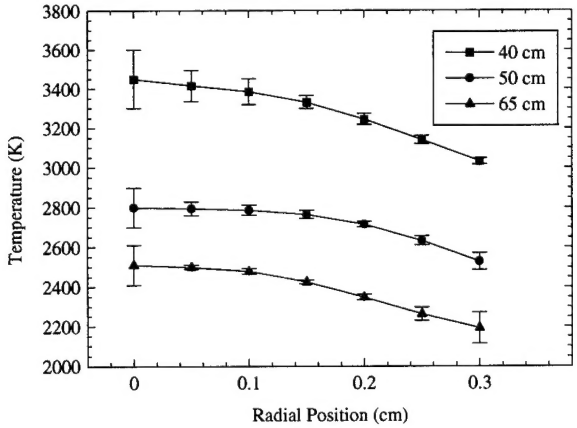

Figure 6. Temperature profiles of the air/argon plasma at 40, 50, and 65 cm downstream of nozzle exit.

Features emanating from the NO A, C, and D states and from the N_2 C state are also visible at these locations. Their shapes are not as sensitive to rotational or vibrational temperature as the OH spectrum but can be used to confirm the deduced temperatures within 500 K. Electronic overpopulation factors are determined in the same manner as for the A state of OH.

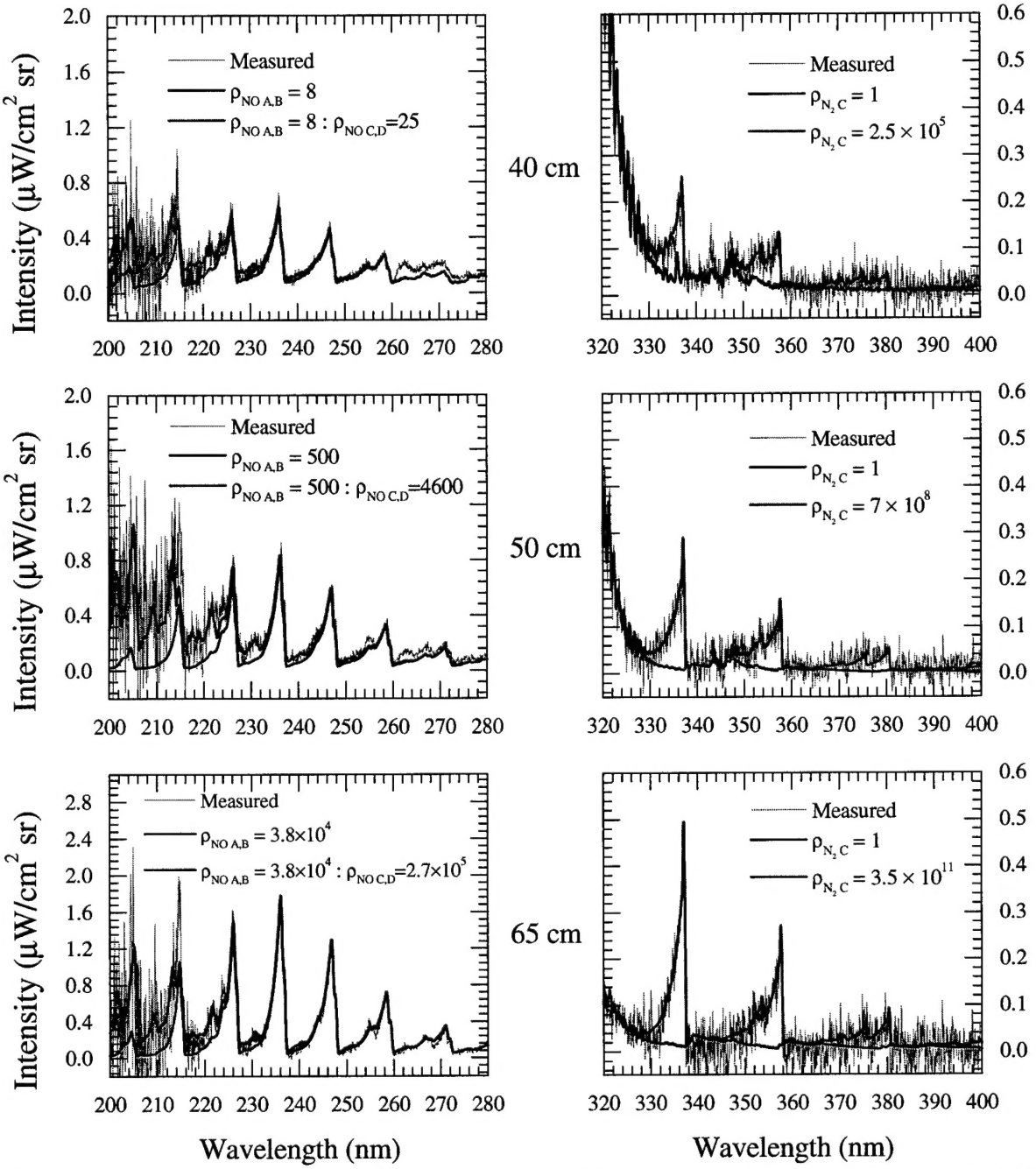

Figure 15. Measured and computed emission spectra of the air/argon plasma at 40, 50, and 65 cm. Included in the spectral simulations are the NO β (B→X), γ (A→X), δ (C→X), ε (D→X), O_2 Schumann-Runge (B→X), N_2 2^+ (C→B), N_2^+ 1^-(B→X), OH (A→X), and NH (A→X) transitions. Unless specified otherwise, the nonequilibrium factors for all species are set equal to 1 in the simulations.

The experimental (gray line) and numerical line-of-sight spectra at the 40, 50 and 65 cm locations are shown in Fig. 7. The region between 280 and 320 nm is excluded as the much more intense OH A-X band (13, 8, and 3 $\mu W/cm^2/sr$ respectively) dwarves the other spectral features. Below 280 nm, the red line in Fig. 7 corresponds to the line-of-sight spectrum obtained by assuming that all electronic levels of NO, except the A and B states, are in LTE at the measured temperature. The NO A state overpopulation, $\rho_{NO\ A}$, is determined by matching the height of the NO γ (0,1) band at 236.2 nm. The blue curve (below 280 nm) accounts for the overpopulation factors of the NO A, C, and D states, with $\rho_{NO\ C}$ determined from the NO δ (0,5) band at 230.8 nm and $\rho_{NO\ D}$ assumed to be equal to $\rho_{NO\ C}$. The NO C and D states are likely to be in equilibrium with each other due to very fast collisional exchange[7,8] owing to the small energy difference between their potential energies. The spectral locations of relevant NO δ and ε transitions are shown in Fig. 8.

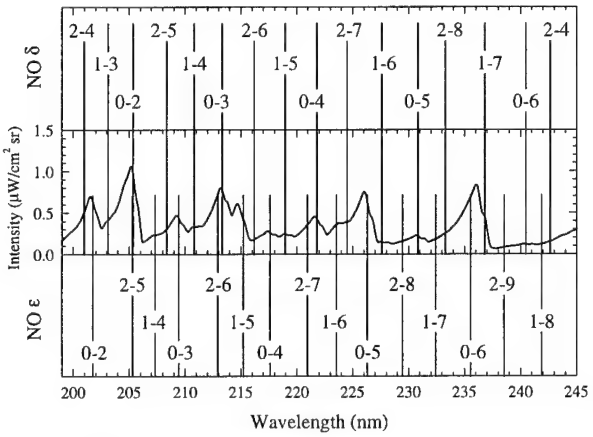

Figure 8. Band origins for NO δ and ε. The spectral emission curve is the non-LTE NEQAIR2 calculation from the 50 cm test section (see Fig. 7).

Above 320 nm, the red curve corresponds to the computed equilibrium spectrum, and the blue curve is obtained by including the measured $\rho_{N_2\ C}$ in the simulation. All measured overpopulation factors are summarized in Table 1.

Table 1. Measured excited state overpopulation factors

Electronic state	Transition name	Term energy (cm^{-1})	ρ 40 cm	ρ 50 cm	ρ 65 cm
NO A	NO γ	43966	8	500	3.8×10^4
NO C	NO δ	52180	25	4600	2.7×10^5
NO D	NO ε	53085	25	4600	2.7×10^5
N_2 C	2+	89137	2.5×10^5	7×10^8	3.5×10^{11}
OH A	A→X	32684	1	4.25	18.3

Kinetic Analysis

The air plasma and nitrogen/argon plasma experiments were used to examine the applicability of the Dunn and Kang,[1] Gupta et al.,[2] and Park[3,4] mechanisms to recombining atmospheric pressure plasmas. As it was concluded that the Park mechanism most adequately described our measurements in pure air,[9,10] only this mechanism will be considered here. The kinetics solver CHEMKIN[11] was used for one-dimensional modeling of the plasma chemistry along the axis of the flow. Rates to describe the relevant hydrogen and argon chemistry, taken from Laux et al.,[9] were appended to the Park mechanism. Rates for O_2[12] and NO[13,14] thermal dissociation by argon were taken from the NIST chemical kinetics database[15] (Table 2). Dissociative and three-body electron attachment reactions such as:

$$O_2 + e \Leftrightarrow O + O^-,$$

$$O_2 + e + e \Leftrightarrow O_2^- + e,$$

while certainly important in low temperature air plasmas,[16] are not considered in the present study because the concentrations of the negative ions are negligible at temperatures above 2000 K. Nor did we consider the N_4^+ dimer formed via the following reaction:[16]

$$N_2 + N_2^+ + M \Leftrightarrow N_4^+ + M,$$

as it is likely to be very unstable in atmospheric pressure gases at temperatures much above room temperature.

Table 2. Forward rate coefficients in Arrhenius form: $A\,T^n \exp(-E/T)$

Reaction	A (cm^3/mol/s)	n	E(K)
$O_2 + Ar \leftrightarrow O + O + Ar$	1.2×10^{14}	0	54280
$NO + Ar \leftrightarrow N + O + Ar$	9.64×10^{14}	0	74697

To calculate centerline velocities, the velocity profiles were assumed to be self-similar to the measured temperature profiles as the Prandtl number was calculated to be near unity. The velocity profiles were then scaled to match the 4.7 g/s mass flow rate of argon/air/hydrogen. The inferred centerline axial velocity was found to decrease from 1060 to 330 m/sec between 0 and 65 cm. The resulting temperature history is displayed in Fig. 9.

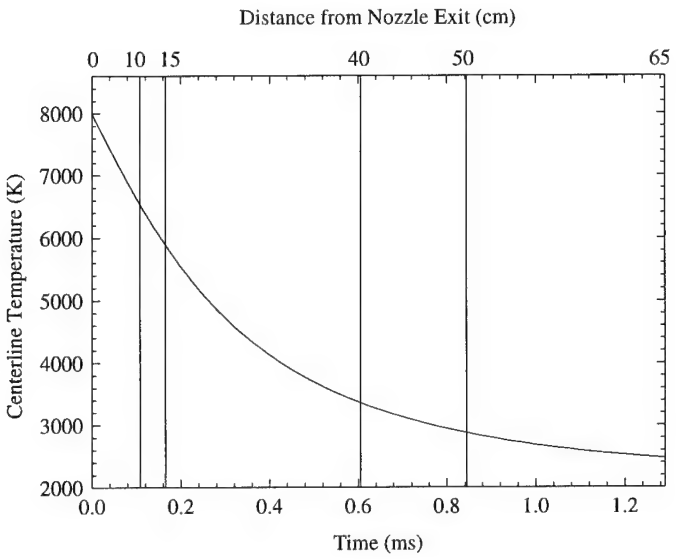

Figure 9. Centerline temperature history based on velocity calculations (air/argon plasma).

To substantiate the velocity predictions, the calculated velocity profiles were used with the measured temperature profiles to calculate the total power in the plasma at each axial location. The calculated decrease in plasma power as a function of distance from the nozzle exit was then compared with calorimetric measurements of the power removed by the water-cooled test sections. Satisfactory agreement is found (Fig. 10).

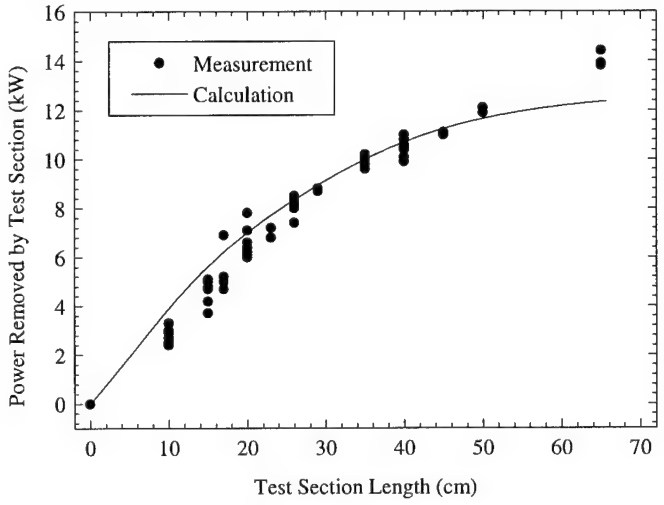

Figure 10. Comparison between measured and calculated power removed by test sections in the air/argon plasma experiments.

The predicted nonequilibrium factors for major species are shown in Fig. 11. The mechanism again predicts that electrons almost exclusively recombine through the fast and equilibrated two body dissociative recombination $NO^+ + e \leftrightarrow N + O$, even though NO^+ is not the dominant ion. Therefore the three body recombination reactions control the electron overpopulation.

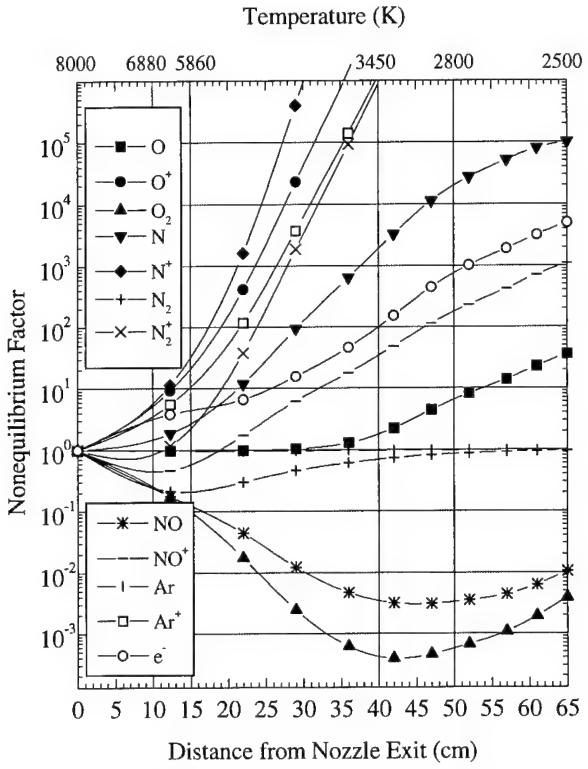

Figure 11. Predicted nonequilibrium factors for the air/argon plasma.

Despite the fact that overpopulation factors have been measured for various molecular *excited* states, situations exist which enable the data to be used to evaluate the accuracy of the chosen *ground state* kinetic mechanism.

The measured NO C state overpopulation, for instance, can be compared with an upper bound value corresponding to the situation where, owing to strong collisional coupling, the C state is in Saha equilibrium with the free electrons. This process corresponds to the following reaction being equilibrated:

$$NO^+ + e + e \leftrightarrow NO\ (C) + e.$$

This equilibrium is described by the Saha relation:

$$\frac{n_{NO^+} n_e}{n_{NO\,C}} = 2\frac{g_{NO^+}}{g_{NO}}\left(\frac{2\pi m_e kT}{h^2}\right)^{3/2}\frac{Z^{vJ}_{NO^+}}{Z^{vJ}_{NO\,C}} e^{-E^{C\lambda}/kT} \qquad (3)$$

where Z^{vJ} represents the rovibrational partition function of the C state of NO or the ground state of NO^+, and $E^{C\lambda}$ is the energy difference between the NO first ionization potential and the C state term energy. The Saha equation can be expressed succinctly as:

$$\rho_{NO\,C} = \rho_{NO^+}\rho_e$$

by dividing each side of Eq. 3 by equilibrium values.

There is another possible mechanism by which the NO C state population can be enhanced. Indeed, the NO C state predissociates and therefore can be populated through inverse predissociation.[17] Given that these rates are fairly large when compared with the rates of C state spontaneous emission and collisional excitation processes,[17] it is reasonable to assume that the reaction

$$NO\ (C) \leftrightarrow N\ (^4S) + O(^3P)$$

is approximately equilibrated. Since this reaction involves ground state N and O atoms, it follows that:

$$\rho_{NO\,C} \cong \rho_N \rho_O \,.$$

It is interesting to note that since Park's mechanism predicts that the dissociative recombination reaction $NO^+ + e \leftrightarrow N + O$ is fast and equilibrated, the following relation holds at all locations:

$$\rho_{NO^+} \rho_e \cong \rho_N \rho_O$$

Thus both Saha coupling and predissociation coupling yield the same predicted upper limit for the overpopulation factor of the NO C state. Numerical predictions for the upper bound on $\rho_{NO\,C}$ are compared with measurements in Fig. 12a. As can be seen in Fig. 12a, the upper bound determined with Park's mechanism appears consistent with the measured overpopulation. However, since it is expected that the coupling due to predissociation/inverse predissociation is very strong for the NO C state, one would expect a closer agreement between the measurements and the predicted upper bound. It would thus appear that ρ_N is too high as ρ_O is relatively close to unity. Furthermore, since the three body recombination of NO accounts for about 38 to 20 % of the total N atom consumption between 15 and 60 cm downstream of the nozzle exit (the balance being due to the Zeldovich reactions whose rates can be considered well known), the rate of $N + O + M \leftrightarrow NO + M$ may be too slow. While Park concludes that this rate is known within a factor three,[3] examination of his compilation of relevant NO thermal dissociation rate measurements seem to warrant a factor ten uncertainty on this rate. Thus, Fig. 12b includes predictions based on calculations in which the third body efficiencies for this reaction, excluding M = Ar, have all been enhanced by a factor ten. (The argon third body efficiency was not enhanced as the rate of thermal dissociation of NO by argon seems to be known well.[15]) It can be seen from Fig. 12 that multiplying the third body efficiencies by a factor 10 improves the agreement between measurements and predictions for test-sections $\leq$45 cm, but produces a recombination rate that is too fast at longer distances. Several issues must be examined in order to draw more definite conclusions about these third body efficiencies. First, a detailed collisional-radiative model is warranted to better determine the degree of coupling between the NO C state and electrons or N and O atoms via the two processes previously mentioned. And second, possible departures from a Maxwellian distribution for the free-electrons and their consequences on rate coefficients should be considered. A preliminary analysis of these effects (see Appendix B) indicates that departures from a Maxwellian distribution may occur at locations > 35 cm. These

various issues are currently being examined in order to provide a better assessment of the rate of NO thermal dissociation.

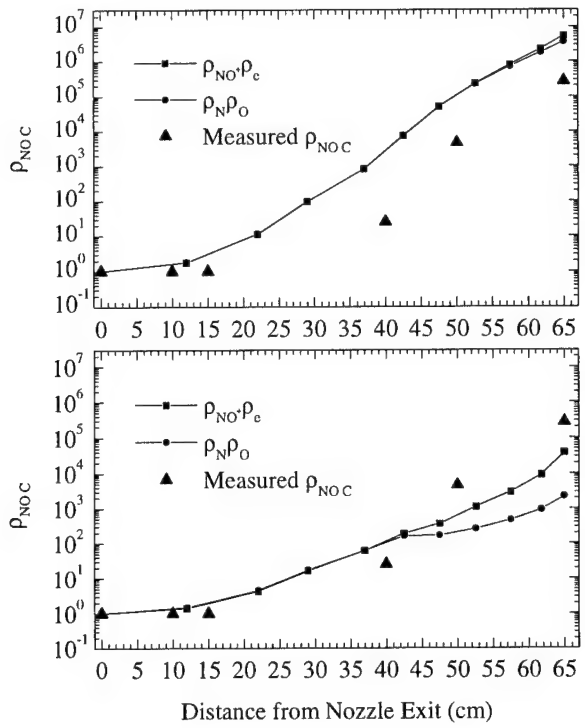

Figure 12. Comparison between calculated and measured NO C state nonequilibrium factors. Top frame (12a) uses Park's mechanism. Bottom frame (12b) uses Park's mechanism with a rate of NO thermal dissociation enhanced by a factor 10.

Similar arguments can be made with regards to the interpretation of the measured N_2 C state overpopulation. If the N_2 C state is in Saha equilibrium with the free electrons, we then have:

$$\rho_{N_2\,C} = \rho_{N_2^+}\rho_e .$$

This equation defines an upper bound for the N_2 C state overpopulation corresponding to full collisional coupling with free electrons. Another upper bound corresponds to equilibrium between the N_2 C state and ground state nitrogen atoms as a result of predissociation and its reverse. This upper bound is defined by:

$$\rho_{N_2\,C} = \rho_N^2 .$$

It should be noted that this is the model employed by the NEQAIR collisional radiative model[18] for the N_2 C state. Figure 13a shows the comparison between the measured N_2 C state overpopulation and the upper bounds just described. As can be seen in Fig. 13a, these two upper bounds do not coincide. This is because Park's mechanism predicts that the dissociative recombination of N_2^+ is not equilibrated. As can also be seen in Fig. 13a, the measured N_2 C state overpopulation is larger than the "upper bound" curve corresponding to predissociation coupling. This may indicate that Saha coupling is stronger

than predissociation coupling for the C state of N_2. (It should be noted that unlike the NO C state, not all rovibrational levels of the N_2 C state predissociate and therefore predissociation coupling may not be as strong as in the case of NO C.) Nevertheless, the upper bound defined by the Saha coupling appears consistent with the measurements. The effect of increasing the third body efficiencies of N + O + M $\leftrightarrow$ NO + M by 10 is shown in Fig. 13b. As was the case for the NO C state analysis, better agreement is obtained between the Saha coupling curve and the measured N_2 C overpopulation at locations $\leq$ 45 cm. Yet it is clear that a more detailed collisional-radiative model is required to interpret the nonequilibrium data.

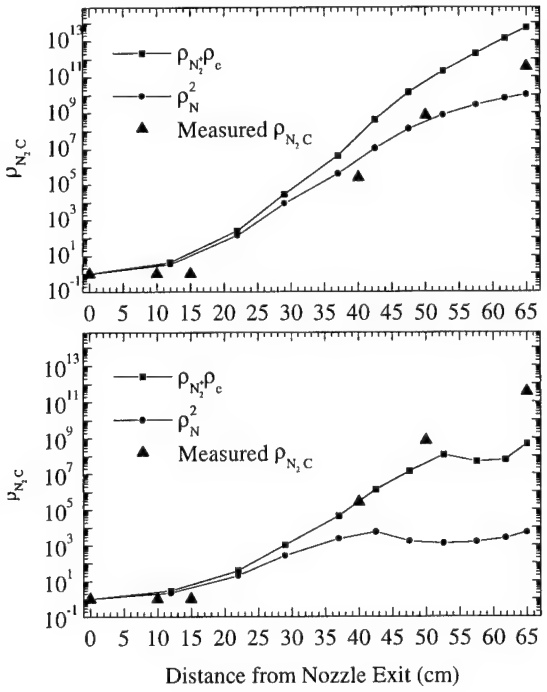

Figure 13. Comparison between calculated and measured N_2 C state nonequilibrium factors. Top frame (21a) uses Park's mechanism. Bottom frame (21b) uses Park's mechanism with rate of NO thermal dissociation enhanced by a factor 10.

Finally we compare the electron overpopulation factors predicted using Park's mechanism with the measured electron overpopulation factors. At 0, 10, and 15 cm, direct measurements of ρ_e were made via the Stark broadening of the H_β line at 486.1 nm. Error bars on these data points (Fig. 14) reflect uncertainties on measured electron number densities and on centerline temperatures. At the exit of longer test-sections, the intensity of the H_β line was very weak, and therefore no direct measurements of electron number densities could be made. However, Park's model predicts that the NO^+ dissociative recombination is equilibrated and that within a factor 3, $\rho_{NO^+} = \rho_e$. It follows that $\rho_{NO\,C}$ should approximately equal $(\rho_e)^2$. Figure 14a compares the predicted electron overpopulation factors and the square root of the measured $\rho_{NO\,C}$. Figure 14b shows the ρ_e predic-

tions obtained if the third body efficiencies mentioned previously are multiplied by 10. This latter curve stops after 42 cm as the $NO^+ + e \leftrightarrow N + O$ reaction is no longer equilibrated. These results support the same conclusions as those drawn from analyzing the NO C and N_2 C state overpopulations.

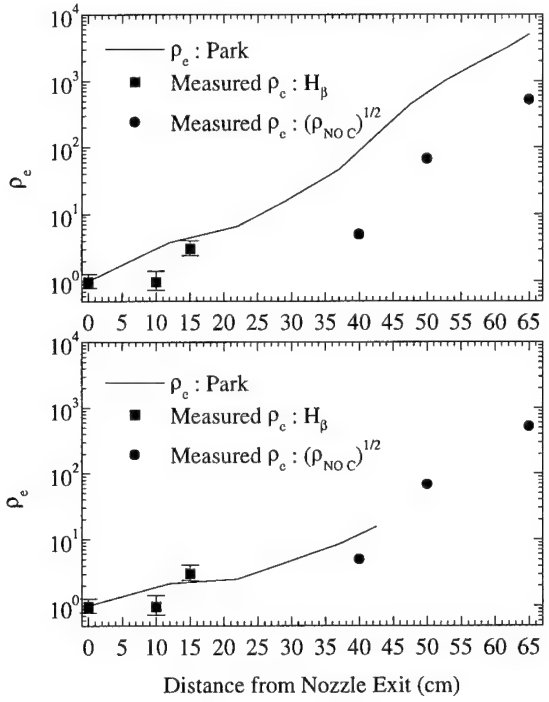

Figure 14. Comparison between calculated and measured electron nonequilibrium factors. Top frame (14a) uses Park's mechanism. Bottom frame (14b) uses Park's mechanism with rate of NO thermal dissociation enhanced by a factor 10.

Conclusion

An analysis of the kinetics of recombining air plasmas was presented. This analysis shows that electron recombination occurs primarily through two-body dissociative recombination reactions. As a result, overall electron recombination rates are significantly greater than those for three-body electron recombination, and the extent of ionizational nonequilibrium is governed by the rates of relatively slow three-body atom recombination reactions such as $N + O + M \rightarrow NO + M$ and $2N + M \rightarrow N_2 + M$. In order to test the predictions of three reaction mechanisms widely used for air plasma chemistry, experiments were conducted with air, nitrogen, and air/argon plasmas in which various degrees of chemical and ionizational nonequilibrium were produced. In all three cases, measurements of electron number densities and excited electronic state concentrations were made in order to assess the recombination models and the rates of the controlling three-body neutral recombination reactions. Predictions based on the model proposed by Park were found to be qualitatively consistent with our observations. Before more quantitative conclusions can be drawn, several issues must be addressed. First, a detailed collisional-

radiative model must be developed to better assess the degree of collisional coupling between electronic excited states and electrons or atoms. Second, the simple one-dimensional model used to predict the time-temperature history of the recombining plasma should be refined. Third, the consequences on the rates of possible departures from a Maxwellian electron energy distribution must be examined.

Nevertheless, it already appears from the present work that all measurements support the proposed air plasma recombination mechanism. In addition, while the rate of three-body N_2 recombination appears to be accurate within a factor 3, our measurements support a rate of three-body NO recombination that is ~10 times faster than the rate proposed by Park and Gupta et al., and ~100 times faster than the rate of Dunn and Kang.

Appendix A. Argon Continuum Radiation

The continuum radiation resulting from electron-ion free-bound (ε_{fb}^{ei}), electron-neutral free-free (ε_{ff}^{en}), and electron-ion free-free (ε_{ff}^{ei}) interactions can in fact be estimated. These three continua correspond to the following processes:

$X^+ + e \leftrightarrow X + h\nu$,

$X + e \leftrightarrow X + e + h\nu$,

$X^+ + e \leftrightarrow X^+ + e + h\nu$,

where X represents Ar, O, N, O_2, N_2, or NO. Argon comprises ninety percent of the plasma in the present experiments and is likely to be the major source of the observed continuum. The argon continuum emission is modeled as follows:[19]

$$\varepsilon = \varepsilon_{fb}^{ei} + \varepsilon_{ff}^{en} + \varepsilon_{ff}^{ei}$$

$$\varepsilon_{fb}^{ei} = C_1 n_e n_i [1 - \exp(-\frac{hc}{\lambda k T_e})] g_i \frac{\xi_{fb}(\lambda, T_e)}{\lambda^2 T_e^{0.5} Z_i}$$

$$\varepsilon_{ff}^{ei} = C_1 n_e n_i \exp(-\frac{hc}{\lambda k T_e}) g_i \frac{\xi_{ff}(\lambda, T_e)}{\lambda^2 T_e^{0.5}}$$

$$\varepsilon_{ff}^{ei} = C_2 n_e n_a \frac{T_e^{1.5} Q(T_e)}{\lambda^2} \left[1 + \left(1 + \frac{hc}{\lambda k T_e} \right)^2 \right] e^{-\frac{hc}{\lambda k T_e}}$$

where $C_1 = 1.631 \times 10^{-43}$ $Wm^4K^{1/2}sr^{-1}$, $C_2 = 1.026 \times 10^{-34}$, n_e, n_a, and n_i are the electron, Ar, and Ar^+ densities, respectively, g_i is the electronic ground state degeneracy of Ar^+, ξ_{fb} the free-bound Biberman factor,[20] Z_i the Ar^+ partition function, ξ_{ff} the free-free Biberman factor, and $Q(T_e)$ the averaged electron-neutral collision cross section. The values of ξ_{fb}, ξ_{ff} and $Q(T_e)$ are specified by Gordon.[21] The results of this model are shown in Fig. A.1 for a 2 mm diameter, uniform temperature, LTE argon plasma. The calculated values of 2.5, 2.4, and 2.2 $\mu W/cm^2/sr$ at 360 nm are consistent with the constants added to the numerical spectrum within a factor 20. Estimates of the contribution from air species to the

recombination continuum are difficult to obtain as we are not aware of calculations and measurements for these quantities at temperatures below 9000 K.[22,23]

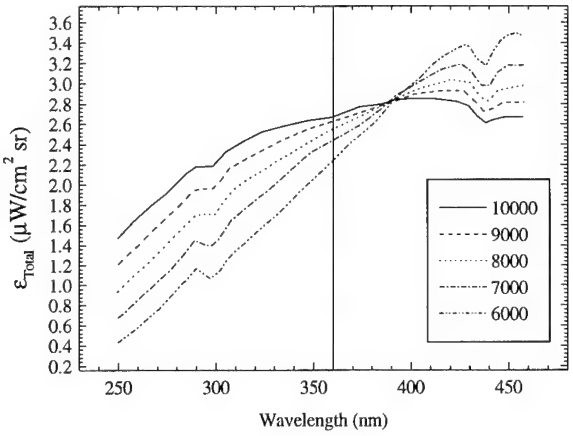

Figure A1. Total radiative recombination emission coefficient for a 1 atm LTE argon plasma. Calculations are for a 2 mm diameter plasma observed through a monochromator with a 0.44 nm instrument broadening.

Appendix B. Electron Energy Distribution

Both the predicted and measured chemical/ionizational nonequilibrium warrant consideration of the validity of applying Park's reaction mechanism to this data analysis. In particular, it is possible that the rates of importance may be dramatically altered by departures from equilibrium in the Maxwellian electron energy distribution upon which Park's rates rest. Sufficient conditions for the existence of a Maxwellian distribution can be obtained by consideration of the first Cartesian-tensor equation formed from the electron Boltzmann equation.[24] In this text, the authors argue that the electron-electron collision integral must be the dominant term in the electron Boltzmann equation if a Maxwellian speed distribution is to exist. An order of magnitude analysis is performed and the following partial list of conditions is derived:

$$\sum_h \frac{m_e}{m_h}\frac{\bar{\nu}_{eh}}{\bar{\nu}_{ee}} << 1 \tag{B1}$$

$$\frac{1}{\bar{\nu}_{ee}\tau} << 1 \tag{B2}$$

$$\frac{\bar{C}_e}{\bar{\nu}_{ee}L} << 1 \tag{B3}$$

$$\left(\frac{U_e}{\bar{C}_e}\right)^2 \frac{\bar{\nu}_{eH}}{\bar{\nu}_{ee}} << 1, \tag{B4}$$

where

$$U_e = \frac{-k}{m_e n_e}\frac{\nabla(n_e T)}{\bar{\nu}_{eh}},$$

$\overline{C}_e$ is the average electron speed; U_e the electron diffusion velocity; $\overline{\nu}_{eh}$ and $\overline{\nu}_{ee}$ the electron-heavy and electron-electron collision frequencies, and τ and L the characteristic time and length scales for macroscopic change. To evaluate these expressions, various assumptions must be made. It is assumed that the electron energy distribution is Maxwellian, so that the average electron speed can be calculated as $(8kT/\pi m_e)^{1/2}$. T is assumed to decrease from 8000 to 2500 K linearly over 65 cm such that $\Delta z/\Delta T \approx 1.2\times10^{-4}$ m/K, where z represents the distance from the nozzle exit. A 100 K temperature drop therefore occurs over 1.18×10^{-2} m. The product (n_eT) is evaluated at LTE conditions. Finally $\nabla(n_eT)$, evaluated over a drop in temperature of 100 K, can be approximated as $\Delta(n_eT)/\Delta z$ where $\Delta z = 1.2\times10^{-2}$ m. The collision frequencies are evaluated with equilibrium number densities and the electron collision cross sections found in Gupta.[2]

The first of these conditions results from the requirement that the electron-electron collision integral be much larger than the electron-heavy collision integral. The next two expressions assure that the plasma is collision-dominated with respect to the electron gas. They state that the time between electron-electron collisions is much less than the characteristic time scale for macroscopic change and that the mean free path for electron-electron collision is much smaller the characteristic length scale of macroscopic change. τ and L are taken as the time to traverse the longest test section (1.29 ms) and the length of this test section (0.65 m), respectively. The final condition requires that the term in the energy equation involving the electric field E' is small compared to the electron-electron collision integral. Numerical evaluations of these conditions are shown in Fig. B1.

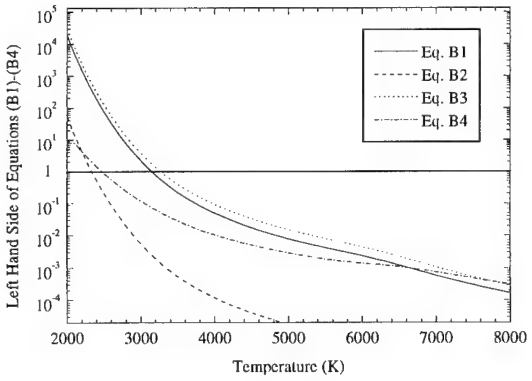

Figure B1. Evaluation of sufficient conditions for the existence of a Maxwellian electron energy distribution.

For temperatures less than ~3800 K, it appears that these sufficient conditions may be violated for an LTE air/argon plasma. It is possible that the observed non-LTE behavior of the air/argon experiments will delay a departure of the electron energy distribution from a Maxwellian. For example, the inferred ρ_e of ~500 at 65 cm (Fig. 22) would increase $\overline{\nu}_{ee}$ and thereby definitely prolong the validity of Eqs. B2 and B3, and possibly Eqs. B1 and B4 depending on the degree of chemical nonequilibrium. Considering both

the approximate nature of these calculations and the fact that these conditions are sufficient but not necessary, a closer examination of the existence or lack of a Maxwellian distribution is justified.

3.3. Significance of the present study

The results from this work have important implications regarding the transport of air plasmas and the development of methods for creating and sustaining elevated non-equilibrium electron number densities in low temperature, atmospheric pressure air. As discussed in this report, the overall recombination of electrons results from and is controlled by the recombination of neutral species. It was already known from our initial studies using existing kinetic mechanisms that the three-body recombination of NO was much faster, by about a factor 10, than the recombination of N_2. From the present work, it appears that NO recombination may be even faster, by about a factor 10, than previously thought. It is clear therefore that in order to maintain elevated electron number densities, the recombination of NO must be inhibited. In future work, particularly in the framework of the newly started Air Plasma Ramparts program, one of our goals will be to explore ways to efficiently sustain air plasmas with highly dissociated NO.

4. Personnel

Professor Charles H. Kruger
Vice-Provost, Dean of Research and Graduate Policy,
Professor, Department of Mechanical Engineering.

Dr. Christophe O. Laux
Research Associate.
(Ph.D. Mechanical Engineering, Stanford University 1993).

Dr. Thomas G. Owano
Senior Research Associate.
(Ph.D. Mechanical Engineering, Stanford University 1991).

Dr. Laurent C. Pierrot
Postdoctoral Fellow
(Ph.D. Ecole Centrale Paris, 1997)

Mr. Richard J. Gessman
Graduate Research Assistant.
(M.S. Aeronautical and Astronautical Engineering, University of Illinois at Urbana-Champaign, 1992).

Mr. Denis Packan
Graduate Research Assistant.
(M.S. Ecole Centrale Paris, France, 1996).

5. Publications

Kruger, C.H., Owano, T.G., and Laux, C.O., "Experimental Investigations of Atmospheric Pressure Nonequilibrium Plasma Chemistry," to appear in the October 1997 special issue of the IEEE Transactions on Plasma Sciences.

Laux, C.O., Gessman, R.J., and Kruger, C.H., "Ionizational Nonequilibrium Induced by Neutral Chemistry in Air Plasmas," *AIAA Journal,* Vol. 34, No. 8, pp. 1745-1747, 1996.

Sarrette, J.P., Gomès, A.M., Bacri, J., Laux, C.O., and Kruger, C.H., "Collisional-Radiative Modeling of Quasi-Thermal Air Plasmas with Electronic Temperatures Between 2000 and 13,000 K—I. $\Theta_e > 4000$ K," *JQSRT*, Vol. 53, No. 2, pp. 125-141, 1995.

Levin, D.A., Laux, C.O, and Kruger, C.H., "A General Model for the Spectral Calculation of OH Radiation in the Ultraviolet," submitted to *JQRST*, 1997.

6. Interactions/Transitions

Laux, C.O., Gessman, R.J., Hilbert, B., Packan, D.M., Pierrot, L.C., and Kruger, C.H., "Infrared Emission of Air Plasmas," Missile Signatures and Aerothermochemistry Meeting, Alexandria, VA, May 12-13, 1997.

Gessman, R.J., Laux, C.O., and Kruger, C.H., "Experimental Study of Kinetic Mechanisms of Recombining Atmospheric Pressure Air Plasmas," AIAA 97-2364, 28th Plasmadynamics and Lasers Conference, June 23-25, Atlanta, GA, 1997.

Candler, G.V., Laux, C.O., Gessman, R.J., and Kruger, C.H., "Numerical Simulation of a Nonequilibrium Nitrogen Plasma Experiment," AIAA 97-2365, 28th Plasmadynamics and Lasers Conference, June 23-25, Atlanta, GA, 1997.

Kruger, C.H., Owano, T.G., Laux, C.O., and Zare, R.N., "Nonequilibrium in Thermal Plasmas," Proceedings of the 23rd International Conference on Phenomena in Ionized Gases, Toulouse, France, July 17-22, 1997 (invited).

Owano, T.G., Laux, C.O., and Kruger, C.H., "Experimental Investigation of Nonequilibrium Plasma Chemistry at Atmospheric Pressure," Proceedings of the 13th International Symposium on Plasma Chemistry, pp. 82-87, August 18-22, Beijing, China.

Gessman, R.J., Laux, C.O., and Kruger, C.H., "Chemical and Ionizational Nonequilibrium in Recombining Atmospheric Pressure Air Plasmas," Gordon Research Conference on Plasma Processing Sciences, New Hampton, NH, August 11-16, 1996.

Laux, C.O., Gessman, R.J., and Kruger, C.H., "Radiative and Kinetic Studies of Nonequilibrium Air and Nitrogen Plasmas," Missile Signatures and Aerothermochemistry Meeting, NASA-Ames Research Center, April 22, 1996.

Laux, C.O., Gessman, R.J., Hilbert, B. and Kruger, C.H., "Infrared Signature Masking by Air Plasma Radiation," NASA-Ames Research Center, Computational Chemistry Seminar Series, April 10, 1996.

Gessman, R.J., Laux, C.O., and Kruger, C.H., "Mechanism for Ionizational Nonequilibrium in Air and Nitrogen Plasmas," Thermosciences Affiliates and Sponsors Conference, Stanford University, February 1996.

Laux, C.O., Gessman, R.J., and Kruger, C.H., "Radiative Phenomena in Nonequilibrium Plasmas," Mechanical Engineering Department Seminar, University of Minnesota, Minneapolis, MN, Nov. 20, 1995.

Laux, C.O., Gessman, R.J., Hilbert, B., and Kruger C.H., "Kinetics and Radiative Studies of Air Plasmas," Computational Chemistry Seminar Series, NASA-Ames Research Center, Moffett Field, CA, August 30, 1995.

Laux, C.O., Gessman, R.J., and Kruger, C.H., "Ionizational Nonequilibrium in Thermal Air Plasmas," Proceedings of the 12th International Symposium on Plasma Chemistry, pp. 753-758, Minneapolis, MN, August 21-25, 1995.

Laux, C.O., Gessman, R.J., and Kruger, C.H., "Mechanisms of Ionizational Nonequilibrium in Air and Nitrogen Plasmas," AIAA Paper 95-1989, 26th AIAA Plasmadynamics and Lasers Conference, San Diego, CA, June 19-22, 1995.

Laux, C.O., Gessman, R.J., Hilbert, B. and Kruger, C.H., "Experimental Study and Modeling of Infrared Air Plasma Radiation," AIAA Paper 95-2124, 30th AIAA Thermophysics Conference, San Diego, CA, June 19-22, 1995.

Levin, D.A., Laux, C.O, and Kruger, C.H., "A General Model for the Spectral Calculation of OH Radiation in the Ultraviolet," AIAA 95-1990, 26th AIAA Plasmadynamics and Lasers Conference, San Diego, CA, June 19-22, 1995.

7. New Discoveries, Inventions, or Patent Disclosures

None

8. Honors/Awards

1997: At the 23rd International Conference on Phenomena in Ionized Gases (Toulouse, France, July 17-22, 1997), Charles H. Kruger gave an invited Plenary Lecture on Non-equilibrium Plasmas and Diagnostics.

1995: At the 12th International Symposium on Plasma Chemistry (Minneapolis, August 1995), the Plasma Chemistry Prize for Best Paper with respect to scientific quality and originality of approach was awarded to Scott K. Baldwin, Thomas G. Owano and Charles H. Kruger for the paper: "Secondary Discharge Induced Nonequilibrium Chemistry in a CVD Diamond DC Arc-Jet," ISPC 12, Conference Proceedings, pp. 2011-2022, Minneapolis, MN, June 21-25, 1995.

9. References

1. Dunn, M.G. and Kang, S.-W., "Theoretical and Experimental Studies of Reentry Plasmas," Report No. NASA CR-2232, 1973.

2. Gupta, R.N., Yos, J.M., Thompson, R.A., and Lee, K.-P., "A Review of Reaction Rates and Thermodynamic and Transport Properties for an 11-Species Air Model for Chemical and Thermal Nonequilibrium Calculations to 30,000 K," Report No. NASA RP-1232, 1990.

3. Park, C., *Nonequilibrium Hypersonic Aerothermodynamics,* Wiley, New York, 1989.

4. Park, C., "Review of Chemical-Kinetic Problems of Future NASA Missions, I: Earth Entries," *Journal of Thermophysics and Heat Transfer*, 7, pp. 385-398, 1993.

5. Laux, C.O., "Optical Diagnostics and Radiative Emission of Air Plasmas," Ph.D. Thesis, Stanford University, 1993.

6. Levin, D.A., Laux, C.O., and Kruger, C.H., "A general model for the spectral calculation of OH radiation in the ultraviolet," *26th AIAA Plasmadynamics and Lasers Conference, AIAA 95-1990*, San Diego, CA, 1995.

7. Callear, A.B. and Pilling, M.J., "Fluorescence of Nitric Oxide. Part 6," *Transactions of the Faraday Society*, 66, pp. 1886, 1970.

8. Lahmani, F., Lardeux, C., and Solgadi, D., "Collision-induced relaxation of NO $C^2\Pi$ (v'=0) and $D^2\Sigma^+$ (v'=0)," *Chemical Physics Letters*, 81, pp. 531, 1981.

9. Laux, C.O., Gessman, R.J., and Kruger, C.H., "Mechanisms of ionizational nonequilibrium in air and nitrogen plasmas," *26th AIAA Plasmadynamics and Lasers Conference, AIAA 95-1989*, San Diego, CA, 1995.

10. Laux, C.O., Gessman, R.J., and Kruger, C.H., "Ionizational Nonequilibrium Induced by Neutral Chemistry in Air Plasmas," *AIAA Journal*, 34, pp. 1745-1747, 1996.

11. Kee, R.J., Rupley, F.M., and Miller, J.A., "Chemkin-II: A Fortran Chemical Kinetics Package for the Analysis of Gas Phase Chemical Kinetics," Report No. SAND89-8009, 1989.

12. Warnatz, J., in *Combustion Chemistry*, edited by W. C. Gardiner, Jr. Springer-Verlag, New York, 1984.

13. Thielen, K. and Roth, P., "Resonance absorption measurements of N and O atoms in high temperature NO dissociation and formation kinetics," *20th Symposium (International) on Combustion, 20*, Ann Arbor, MI, 1984 (Combustion Institute), pp. 685.

14. Tsang, W. and Herron, J.T., "Chemical kinetic data base for propellant combustion. I. Reactions involving NO, NO_2, HNO, HNO_2, HCN and N_2O," *Journal of Physical and Chemical Reference Data*, 20, pp. 609-663, 1991.

15. Mallard, W.G., Westley, F., Herron, J.T., and Hampson, R.F., "NIST Chemical Kinetics Database - Ver. 6.0," , , pp. , 1994.

16. Kossyi, I.A., Kostinsky, A.Y., Matveyev, A.A., and Silakov, V.P., "Kinetic Scheme of the Nonequilibrium Discharge in Nitrogen-Oxygen Mixtures," *Plasma Sources Science and Technology*, 1, pp. 207-220, 1992.

17. Laux, C.O., Gessman, R.J., and Kruger, C.H., "Modeling the UV and VUV Radiative Emission of High-Temperature Air," *28th AIAA Thermophysics Conference, AIAA 93-2802*, Orlando, FL, 1993.

18. Park, C., in *Thermal Design of Aeroassisted Orbital Transfer Vehicles*; *Vol. 96*, edited by H. F. Nelson American Institute of Aeronautics and Astronautics, 1985.

19. Wilbers, A.T.M., Kroesen, G.M.W., Timmermans, C.J., Schram, D.C., "The continuum emission of an arc plasma," *JQSRT*, 45, pp. 1-10, 1991.

20. Biberman, L.M., Norman, G.E., and Ulyanov, K.N., "On the calculation of photoionization absorption in atomic gases," *Optics and Spectroscopy*, 10, pp. 297-299, 1961.

21. Gordon, M.H., "Nonequilibrium effects in a thermal plasma," Ph.D. Thesis, Stanford University, 1992.

22. Morris, J.C., Krey, R.U., and Garrison, R.L., "Bremsstrahlung and recombination radiation of neutral and ionized nitrogen," *Physical Review*, 180, pp. 167-183, 1969.

23. Riviere, P., Soufiani, A., Perrin, M.Y., Riad, H., and Gleizes, A., "Air mixture radiative property modelling in the temperature range 10,000-40,000 K," *JQSRT*, 56, pp. 29-45, 1996.

24. Mitchner, M. and Kruger, C.H., *Partially Ionized Gases,* John Wiley & Sons, Inc., New York, 1973.